ce/papers Proceedings in civil engineering

Ernst & Sohn A Wiley Brand

ORIGINAL ARTICLE

eurosteel AMSTERDAM 2023

Ernst & Sohn A Wiley Brand

Experimental evaluation of the load-bearing capacity of steel-reinforced CFST stub columns under a fire scenario

David Medall[1] | Carmen Ibáñez[1] | Ana Espinós[1] | Manuel L. Romero[1]

Correspondence

Dr. Ana Espinós
Associate Professor
ICITECH
Universitat Politècnica de València
Camino de Vera, s/n
46022 Valencia (Spain)
Email: aespinos@mes.upv.es

[1] ICITECH, Universitat Politècnica de València, Spain

Abstract

Composite construction is becoming increasingly used across the world, since it enables to exploit the benefits of steel and concrete working together, leading to cost-effective solutions. Recent technological developments have facilitated the introduction of new typologies, which combined with the use of high performance materials allow for significant load-bearing capacities with reduced cross-sectional dimensions. One of these innovative composite sections are the so-called steel-reinforced concrete-filled steel tubular (SR-CFST) columns, where an open steel profile is embedded into a CFST section. Apart from the broadly recognized benefits of these typologies at room temperature, they show an enhanced fire performance due to the inherent fire protection offered by the surrounding concrete to the inner steel profile, which delays its loss of mechanical capacity at elevated temperatures. However, the experimental evidence on the fire behaviour of SR-CFST columns is still scarce, being much needed for the development of specific design provisions that consider the use of the inner steel profile in CFST columns.

In this paper, a new testing program on the thermo-mechanical behaviour of SR-CFST columns is presented to extend the available experimental database. A cylindrical electric furnace attached to a loading rig equipped with a 5000 kN hydraulic jack is used. In total six SR-CFST stub columns are tested, three circular and three square sections, combining high strength steel and concrete.

Keywords

Concrete-filled steel tubular columns, Embedded steel profile, High strength steel, High strength concrete, Fire resistance

1 Introduction

Comprised of hollow steel tubes filled with concrete and an embedded steel profile, steel-reinforced concrete-filled steel tubular (SR-CFST) columns may be considered to be a natural variation of the conventional CFST columns. Due to the combined action of steel and concrete, CFST columns are widely known by their exceptional qualities, one of them being their excellent fire resistance. In SR-CFST columns the fire behaviour may be enhanced due to the protection that the concrete core offers to the embedded steel profile, thus delaying its degradation. Under fire conditions, the column may resist the applied load for an extended period of fire exposure time.

Amongst the scarce experimental investigations available on SR-CFST columns exposed to fire conditions, one can find the tests performed at the University of Liège [1] or those carried out in Shanghai [2,3]. More recently, the experiments conducted at Southeast University [4-6] must be highlighted where specifically SR-CFST columns with a cruciform steel section embedded in the concrete were tested subjected to uniform and non-uniform heating and with and without fire protection. In light of the review of the experimental programmes published in the literature, it can be seen that the number of available fire test results on SR-CFST columns is still limited.

Based on the previous investigations and with the aim of extending the available experimental data, this work presents a series of elevated temperature tests performed on stub columns. New aspects, not investigated in the previous experimental campaigns, such as the use of high strength steel at the embedded profile and high strength concrete as infill are covered in this research to ease the understanding of the performance of these columns under a fire situation.

2 Experimental program

2.1 Definition of test specimens

In this experimental program, six SR-CFST specimens

were tested, which were grouped into two series comprising circular and square geometries respectively (see Figure 1a) and 1b).

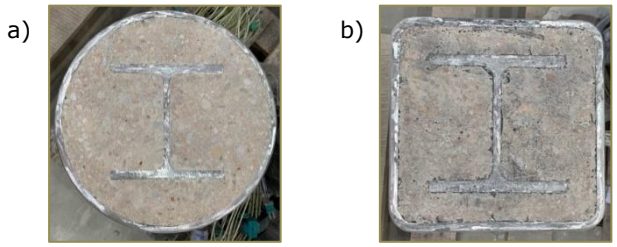

Figure 1 SR-CFST configurations tested: a) circular; b) square.

For the sake of comparison, the cross-sectional area of steel the circular and square steel tubes utilised was the same (with a maximum difference of a 0.57%). Additionally, two hollow steel tubes (one circular and one square) with the same dimensions as the ones utilized for conforming the SR-CFST specimens were tested as a reference for comparison.

For the circular columns, ϕ273x6.3 mm hollow steel tubes were employed, while the square steel tubes were #220x6.3 mm. For the embedded steel profiles, HEB140 sections were used. All the columns had a length of 600 mm.

In Table 1, the cross-sectional properties of all tested specimens and other data corresponding to each series are summarized.

For convenience, the test specimens were named as follows: SR-CFST-S-TMi (i.e. SR-CFST-C-TM1), where S stands for the cross-sectional shape of the outer steel tube (C for circular and S for square) and TMi represents the number of test, each of them with a different combination of grades for the steel of the embedded profile and concrete infill. For the hollow steel tube tests, designation CHS and SHS followed by the label TM0 indicative of a reference case was used.

2.2 Material properties

Steel

In this experimental program, all the hollow steel tubes were cold-formed carbon steel of grade S355. Regarding the embedded steel profiles, in four of the columns hot-rolled sections of normal strength steel grade S275 were used, while for the other four columns, the inner profiles were fabricated from welded high strength steel plates of grade S700MC. For all the hollow steel tubes and embedded steel profiles, the actual values of the yield strength (f_{yo} and f_{yi}, respectively) and the ultimate strength (f_{uo} and f_{ui}, respectively) were determined through the corresponding coupon tests (three tests per tube), the average value being shown in Table 1.

Concrete

Sets of three cylindrical and three cubic samples for each type of concrete mix used for filling the column specimens were prepared in a planetary mixer and cured in standard conditions for 28 days. In order to obtain the actual concrete strength (f_c), the pertinent uniaxial compression tests were performed before the start of the experimental program. The moisture content of the concrete samples was also obtained following a standard procedure according to ISO 12570:2000 [7], giving the results shown in Table 1.

Table 1 Details of the tested specimens.

Specimen	D or B (mm)	t_o (mm)	f_{yo} (MPa)	f_{uo} (MPa)	f_{yi} (MPa)	f_{ui} (MPa)	f_c (MPa)	Moisture (%)	Load (kN)	FT (min)
CHS-TM0	273	6.3	413.33	483.28	-	-	-		1020.7	63
SR-CFST-C-TM1	273	6.3	413.33	483.28	315	441	29.73	6.28	2812.3	267
SR-CFST-C-TM2	273	6.3	413.33	483.28	777.2	853.68	29.73	6.28	3488.9	405
SR-CFST-C-TM3	273	6.3	413.33	483.28	315	441	86.16	2.11	3936.8	317
SHS-TM0	220	6.3	495.84	549.65	-	-	-		1154.3	43
SR-CFST-S-TM1	220	6.3	495.84	549.65	315	441	29.73	6.28	2377.4	239
SR-CFST-S-TM2	220	6.3	495.84	549.65	777.2	853.68	29.73	6.28	3097.9	308
SR-CFST-S-TM3	220	6.3	495.84	549.65	315	441	86.16	2.11	3306.5	285

Note: D and B are the outer diameter or dimension for circular and square sections respectively; t_o is the outer steel tube thickness; f_{yo} and f_{yi} are the yield strength of steel for the outer steel tube and inner embedded section respectively; f_{uo} and f_{ui} are the ultimate strength of steel for the outer steel tube and inner embedded section respectively; f_c is the concrete cylinder compressive strength; and FT is the failure time.

2.3 Specimens preparation

All the columns were prepared and tested at the Concrete Science and Technology Institute (ICITECH), at Universitat Politècnica de València (Spain). At both ends of each specimen, steel plates with dimensions 300x300x10 mm were placed. First, a steel plate was welded to the bottom of the embedded steel profile. Next, the thermocouples were positioned together with the hollow steel tube in order to correctly place the wires. A hole was drilled at the lower part of the outer steel tube for this purpose and to allow vapour ventilation during heating. Later, the bottom of the hollow steel tube was welded to the steel plate. Once the column was filled with concrete and it was settled with the help of a needle vibrator, the specimen was covered with a plastic film. Finally, the second plate was welded to the top end of the column right after smoothing

the top surface in order to assure planarity and the contact of the steel plate with all the components.

The thermocouples layout is presented in Figure 2. A set of 10 thermocouples were positioned at the mid-length of the section to register the temperature evolution during the tests. The arrangement was as follows: thermocouples number 1 and 6 were welded to the outer steel tube surface; thermocouples number 7, 8, 9 and 10 were welded at different points of the embedded steel profile; thermocouples number 2, 3 and 4 were embedded in the concrete core and placed equidistantly, with a separation of 1/6 of the section width; and thermocouple number 5 was also embedded and positioned at 1/4 of the section width.

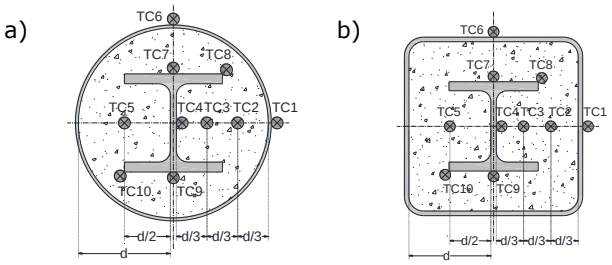

Figure 2 Layout of thermocouples: a) circular sections; b) square sections.

2.4 Test setup and procedure

A thermo-mechanical testing protocol was designed, where a sustained load was applied to the SR-CFST specimens, being simultaneously heated inside an electrical furnace.

For that purpose, a vertical testing frame equipped with a hydraulic jack of 5000 kN capacity was employed (Figure 3). A 40% of the ultimate capacity of the columns at room temperature (see values in Table 1) was applied concentrically to their top end through a spherical bearing, while the bottom end of the columns was attached to the testing rig through a bolted plate. Once the desired load was applied, it was kept constant and the heating of the specimen started, with unrestrained column elongation.

A small electric furnace of 10000 W power was coupled to the testing rig, see Figure 3. The furnace had an inner diameter of ϕ400 mm, consisting of two semicylinders joined by a hinge. As can be seen in Figure 4, the electric elements of the refractory wall of each semicylinder were distributed evenly in parallel layers through the whole length for both sides. To guarantee the uniformity of the heating through measurements of the furnace inner temperature, three thermocouples were evenly distributed inside the furnace chamber along its height. Once the furnace was closed and the specimen ready for testing, the open cavities at the top and bottom ends of the furnace were covered with fibre blanket, in order to minimise the heat loss. A purpose-made protective hood was attached to the top end of the column to prevent the load cell from receiving the convective heat flow. Additionally, the contacting plates at the top end of the column were thermally insulated with layers of fibre blanket to avoid the possible heat conduction towards the load cell.

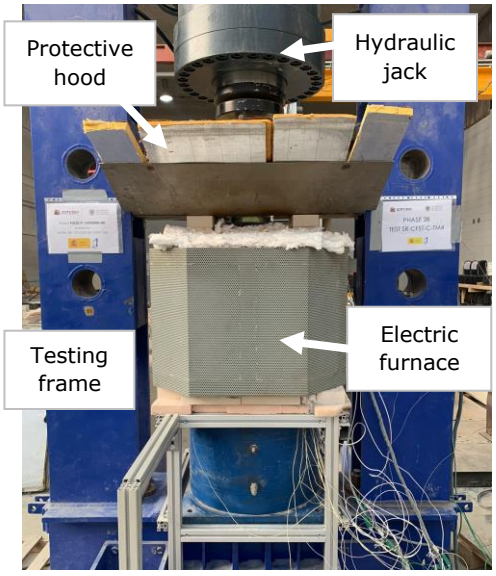

Figure 3 General view of the test setup.

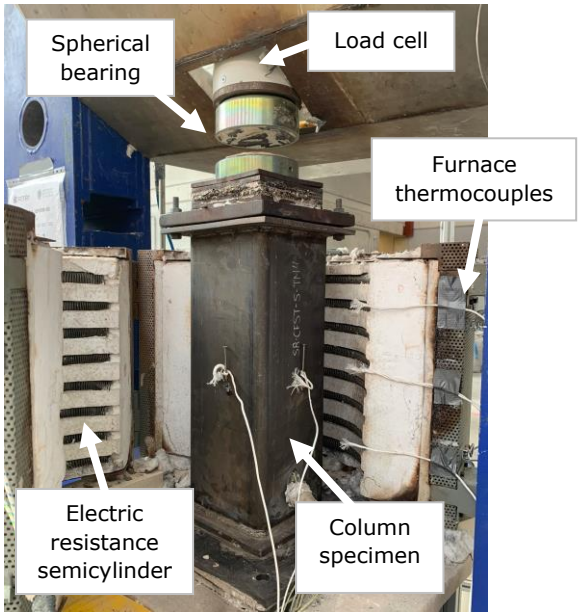

Figure 4 Specimen prepared for testing inside the electric furnace.

A transient heating regime was applied in the thermo-mechanical tests, with a non-constant heating rate. The electric furnace power target was set to its maximum according to the manufacturer specifications, although due to its high inertia at the first stages of heating and the massive size of the tested stub column specimens, the standard ISO-834 temperature-time curve was not reached in the tests. This fact justifies that all the comparisons and discussion of results presented in this work refers to "failure times", rather than "standard fire resistance times".

3 Test results and discussion

3.1 Cross-sectional temperature evolution

In Figure 5, the registered temperatures during the heating process are shown. For the sake of clarity only the data of five of the thermocouples are displayed together with the evolution of the furnace temperature.

For the square SR-CFST columns temperatures were generally higher than for the corresponding circular columns, which may be explained with the effect of the section factor, i.e. for the same cross-sectional area, the square sections present a higher exposed perimeter.

For both series, the delay of temperature rise at the inner steel profile can be observed. The thermal protection provided by the outer steel tube together with the low thermal diffusivity of concrete are responsible for this effect.

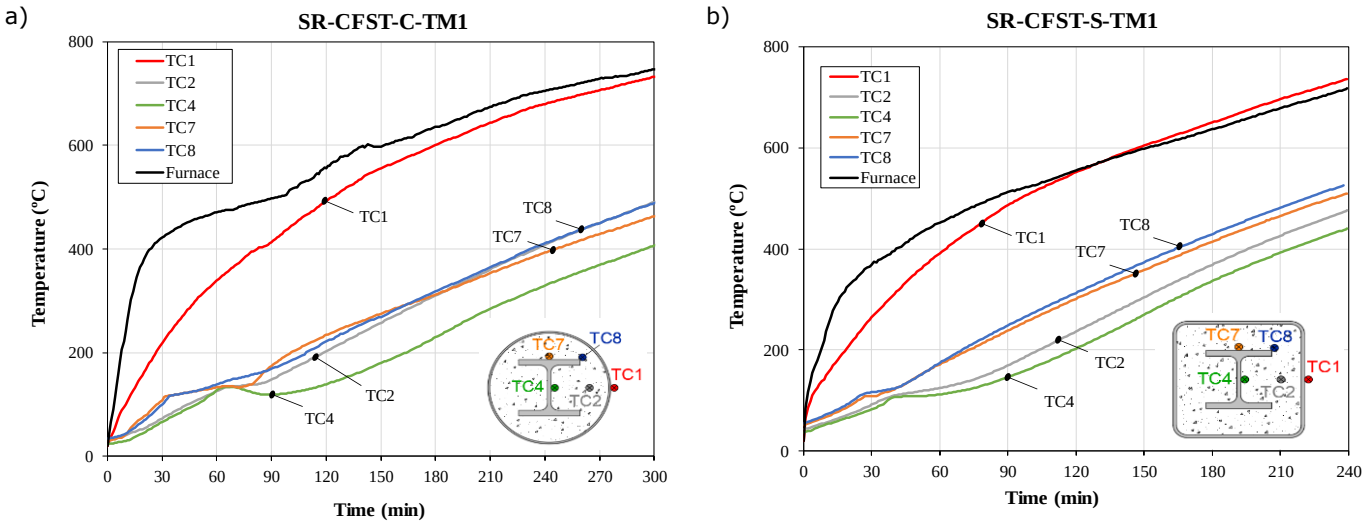

Figure 5 . Cross-sectional temperatures for two of the tested specimens: a) circular section; b) square section.

3.2 Failure modes

Figure 6 displays visually the state of all the columns after the thermo-mechanical tests. As shown in this figure, the outer steel tubes experienced local buckling around their mid-sections, which was more evident for the hollow tubes. In the case of the SR-CFST columns, the local buckling was more notable for the square specimens.

During the tests, the evolution of the axial displacement at the top end of the column was monitored and recorded by means of the load cell, showing a first stage dominated by the expansion of the outer tube; a second stage with a gradual shortening of the column after the degradation of the outer tube; and the end of the test when eventually the defined failure criterion is met.

A homogenous criterion was defined for determining the failure time of the columns based on EN 1363-1 Section 11.1(b) [8] where, for vertical members in compression, failure is established when any of the following two criteria is met:

- Vertical contraction limit: h/100 mm
- Contraction velocity limit: 3h/1000 mm

where h is the initial length of the column. Therefore, the maximum contraction allowed for the tested columns was set to 600/100 = 6 mm and the maximum contraction velocity was set to 3×600/1000 = 1.8 mm/min. For all the SR-CFST tests, the first criterion was met earlier, while for the hollow tube tests, the second criterion was reached sooner.

In Figure 7, the graphs show the evolution of the axial displacement along the heating time for both series of columns. At the first stage of the heating, due to the direct exposure to the heat source and the higher thermal expansion of steel as compared to the concrete infill, the outer steel tube supports alone the applied load for a certain amount of time until yielding. After its loss of capacity, the load is transferred to the inner parts of the section, which owing to the higher thermal capacity of the concrete infill, heat up slower and are therefore able to sustain the load for a significant period of time, until eventually the degradation of concrete and the inner steel profile occurs, stage where the column axial displacement gradually decreases, as a sign of capacity loss.

3.3 Comparison of the thermo-mechanical performance of the different cases analysed

In general, the circular SR-CFST specimens were able to sustain the applied load for a longer heating time than their square counterparts. For each series, the failure time significantly increased when using high strength steel at the inner profile, and a certain enhancement was also obtained with the use of high strength concrete.

It can also be observed that the hollow tubes had a much lower failure time than the SR-CFST columns. Their premature failure is due not only to the reduced mechanical capacity triggered by the local buckling of the tube wall, but also to the extremely fast heating of the section. Given the lack of concrete filling, the phenomenon of heat dissipation that benefits the SR-CFST columns does not occur, leading to a sharp increase of temperatures in the steel tube.

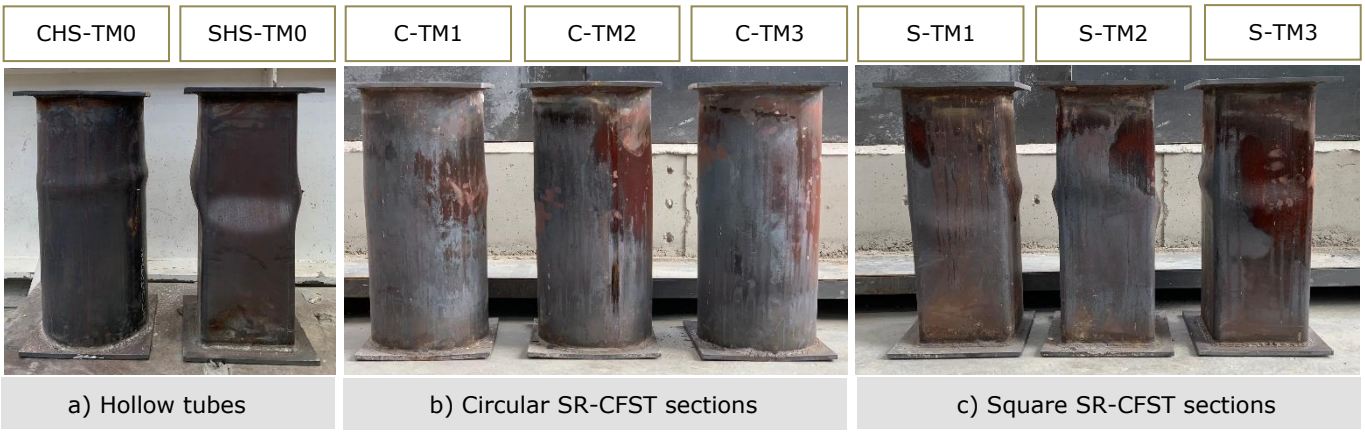

Figure 6 . Columns after test.

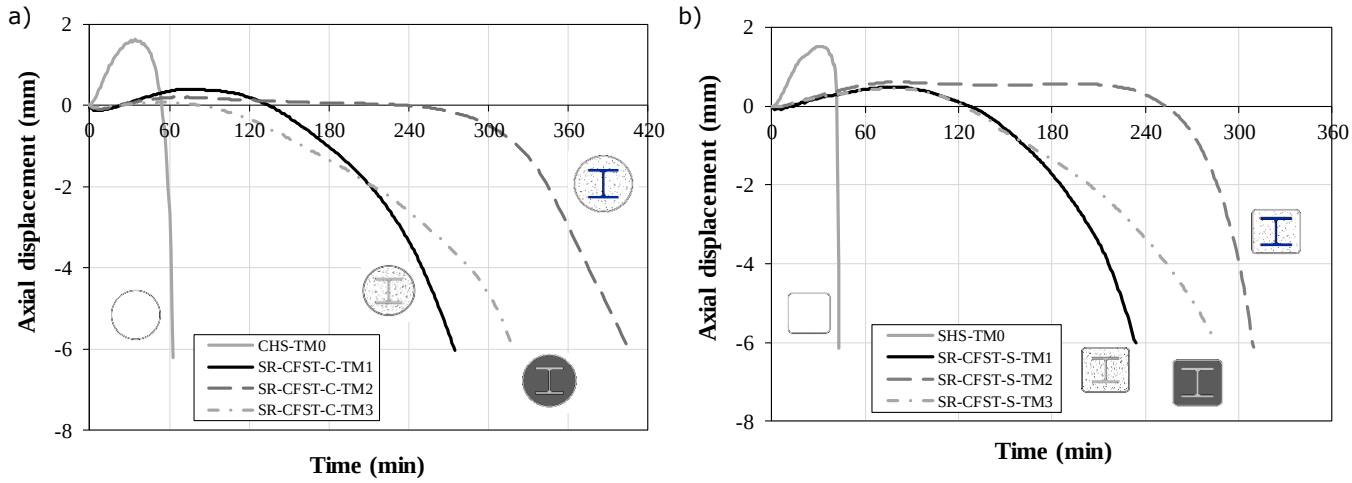

Figure 7 . Axial displacement versus time curves: a) circular sections; b) square sections.

4 Assessment of the failure time of SR-CFST stub columns under fire

Since one of the objectives of this work is to assess the influence that the high performance materials have on the failure time of the SR-CFST columns, an analysis of the mechanical contribution of the different configurations of materials obtained from the experimental results is conducted in this section.

In the investigations related to CFST columns it is common to use these parameters and taking as a basis the same concept, a new mechanical ratio can be defined: the high performance ratio (HPR).

Taking into account that the expected enhanced mechanical behaviour of a SR-CFST column with high performance materials (in this program specimens TM2 and TM3 for both series, circular and square) with respect to a SR-CFST column with normal strength materials is due precisely to the presence of high strength concrete or high strength steel, the HPR is calculated as the ratio between the failure time achieved by a column of each series ($FT_{C\text{-}TMi}$ or $FT_{S\text{-}TMi}$) with respect to the failure time measured for the TM1 column of the corresponding series, which will serve as reference ($FT_{C\text{-}TM1}$ or $FT_{S\text{-}TM1}$). Therefore, a value greater than unity means that the contribution of the high performance materials is positive.

For circular SR-CFST columns:

$$HPR_{Ci} = \frac{FT_{C-TMi}}{FT_{C-TM1}} \quad (1)$$

And for square SR-CFST columns:

$$HPR_{Si} = \frac{FT_{S-TMi}}{FT_{S-TM1}} \quad (2)$$

The values obtained for this ratio are shown in Table 2 and in Figure 8, which may help to quantify the trend observed previously through the load-deflection curves.

Table 2 HPR for the different tested specimens.

Specimen	FT (min)	HPR
SR-CFST-C-TM1	267	-
SR-CFST-C-TM2	405	1.52
SR-CFST-C-TM3	317	1.19
SR-CFST-S-TM1	239	-
SR-CFST-S-TM2	308	1.29
SR-CFST-S-TM3	285	1.19

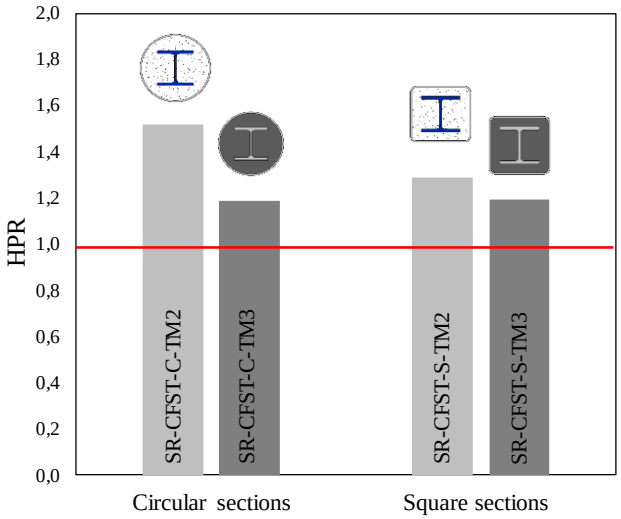

Figure 8 HPR for both series of tested SR-CFST columns.

In view of the values of the HPR, it is clear that using high strength steel in the inner steel section is the most effective strategy to enhance the fire response of stub SR-CFST columns, especially in circular columns. This may be explained because the circular shape offers the columns a better thermal behaviour (lower section factor) and due to the effect of partial confinement, which should be confirmed by means of further numerical investigations.

However, in both TM3 specimens, the response is mainly controlled by the concrete infill, highly influenced by its moisture content, which according to the measured values was slightly lower for the high strength concrete mixture as compared to the normal strength one, therefore producing a faster heating of the section. Note that with the same moisture content the benefits of filling the SR-CFST columns with high strength concrete would have been even more notable.

5 Conclusions

Through the experimental investigation described in this paper, the thermo-mechanical response of stub SR-CFST columns has been studied. The evolution of the cross-sectional temperatures with time and the axial displacement versus time histories were analysed. Six SR-CFST specimens were tested. First, the columns were loaded at a certain load level and afterwards uniformly heated inside an electric furnace until failure. According to their external shape, the columns were grouped into two series comprising circular and square geometries respectively and, for the sake of comparison, the selected circular and square steel tubes had a comparable steel usage. From this study, some conclusions can be drawn:

• Temperatures were generally higher for the square SR-CFST columns than for the corresponding circular columns, which may be due to the effect of the higher section factor of square columns as compared to their circular counterparts.

• The circular specimens reached higher failure times than the square columns. The failure time significantly increased with the use of high strength steel at the embedded steel profile, as well as with the use of high strength concrete as infill.

Acknowledgements

The authors would like to express their sincere gratitude for the help provided through the Grant PID2019-105908RB-I00 and for the first author's pre-doctoral contract through the Grant PRE2020-093106 funded by MCIN/AEI/ 10.13039/501100011033 and by "ESF Investing in your future". The authors are deeply grateful to Dr Enrique Serra for his help and assessment to prepare and conduct the experiments and Dr Andrés Lapuebla-Ferri and Dr David Pons for their help in conducting the material tests.

References

[1] Dotreppe, J.C.; Chu, T.B.; Franssen, J.M. (2010) *Steel hollow columns filled with self-compacting concrete under fire conditions*. Proceedings of the 3rd Congress of the International Federation for Structural Concrete (FIB) and PCI Conference.

[2] Meng, F.Q.; Zhu, M.C.; Clifton, G.C.; Ukanwa, K.U.; Lim, J.B.P. (2020) *Performance of square steel-reinforced concrete-filled steel tubular columns subject to non-uniform fire*. J Constr Steel Res 166, 105909.

[3] Meng, F-Q.; Zhu, M-C.; Clifton, G.C.; Ukanwa, K.U.; Lim, J.B.P. (2021) *Fire performance of edge and interior circular steel-reinforced concrete-filled steel tubular stub columns*. Steel Compos Struct 41, 115-22.

[4] Mao, W.J.; Wang, W.; Zhou, K.; Du, E.F. (2021) *Experimental study on steel-reinforced concrete-filled steel tubular columns under the fire*. J Constr Steel Res 185, 106867.

[5] Mao, W.J.; Wang, W.; Zhou, K. (2022) *Fire performance on steel-reinforced concrete-filled steel tubular columns with fire protection*. J Constr Steel Res 199, 107580.

[6] Mao, W.J.; Zhou, K.; Wang, W. (2023) *Investigation on fire resistance of steel-reinforced concrete-filled steel tubular columns subjected to non-uniform fire*. Eng Struct 280,115653

[7] ISO 12570:2000. *Hygrothermal performance of building materials and products — Determination of moisture content by drying at elevated temperature*. International Organization for Standardization.

[8] EN 1363-1:2020. *Fire resistance tests - Part 1: General requirements*. Brussels, Belgium: Comité Européen de Normalisation.